New modular assays for the quantitative study of skylight navigation in flying flies

Thomas Mathejczyk and Mathias F. Wernet*

Freie Universität Berlin
Fachbereich Biologie, Chemie und Pharmazie
Institut für Biologie – Neurobiologie
Königin-Luise Strasse 1-3
14195 Berlin, Germany

*: Corresponding author
e-mail: mathias.wernet@fu-berlin.de
phone: +49-30-838-60115

Summary

The quantitative study of visual behaviors using virtual flight arenas is complicated by the fact that an effective experimental setup needs to combine a rather complex set of custom-built mechanical, electronic, and software components. Assembling such an apparatus amounts to a major challenge when working in an environment without the support of a machine shop. Here we present detailed instructions for the assembly of virtual flight arenas optimized for *Drosophila* skylight navigation, which can easily be modified towards other uses. This system consists entirely of off-the-shelf parts and 3D-printed components, combining a modular flight arena designed to reduce visual artifacts, swappable high-power LED light sources, polarization filters on a computer-controlled rotating filter wheel, all placed within a temperature and humidity controlled environment. Using this new assay, we show that individual flies choose arbitrary headings when flying under a uniform field of linear polarization. Furthermore, flies adjust their heading to both sudden and continuous changes in filter orientation and can keep their chosen heading for several minutes. Finally, flies show the tendency to maintain headings even after interruption with an unpolarized stimulus. Taken together, these findings demonstrate the usefulness of these assays for the study of skylight navigation in flies.

Introduction

The quantitative study of visual behaviors using single flies suspended in a virtual flight arena has long served as a powerful method for probing photoreceptor function, behavioral mechanisms, as well as the computational role of underlying circuit elements[1-3]. First established using larger insects, these assays have become particular useful in the dissection of visual circuitry in *Drosophila melanogaster*, by taking advantage of its unique molecular genetic toolkit[1]. Since early adaptations to *Drosophila*[4, 5], virtual flight arenas have been used to quantify behavioral responses to a multitude of visual stimuli, ranging (for example) from moving edges, different colors, celestial bodies, learned shapes, to more complex visual scenes[6-12]. Visual responses of flying *Drosophila melanogaster* to linearly polarized light emanating from above (thereby simulating the celestial polarization pattern) using a flight simulator have also been demonstrated[13-15]. In these experiments, flies are presented a linearly polarized stimulus which, in many cases can be generated using commercially available polarization filters[16]. Fairly little is known about the navigational capabilities of free-living fruit flies, yet catch-and-release experiments suggest that several *Drosophila* species are able to keep straight headings over extended periods of time, while flying in desert environments which few visual landmarks (reviewed in[17]). Skylight navigation experiments using virtual flight arenas therefore serve as an attractive platform for the quantitative study of the navigation skills of both wild type insects, as well as of specimens harboring well-defined circuit perturbations.

So far, the assembly of a virtual flight arena for studying skylight navigation in flying flies required the combination of very specific skill sets ranging from the construction and assembly of both mechanical and electrical parts, as well as programming of the codes necessary for the motorized rotation of the polarization filter. In addition, tight control over ambient temperature and humidity are crucial[18], both for reproducible wild type behavior, as well as for certain genetic perturbations. Assembly of such a complicated apparatus is a major challenge when working at a research institution without a dedicated work shop, a problem that becomes more immanent with many University departments discontinuing such services. Alternatively, the purchase of custom-made off-the-shelf options remains rather costly and cannot easily be fit into a realistic research budget. The recent development of affordable 3D filament printers combining both fast and precise printing performance with a choice of cheap and swappable printing materials for different applications now offers an attractive solution for generating new and affordable, quantitative assays for studying anatomy, behavior and physiology of different model organisms[19, 20]. Furthermore, an interactive community of researchers producing and sharing both 3D printing instructions as well as software codes for related robotic applications has now made it possible that such assays can now be introduced in a large scale in schools and Universities, both in developed and developing countries.

Here we present detailed instructions for the assembly of virtual flight arenas optimized for, but not limited to studying skylight navigation in *Drosophila*. These instructions include: (1) a detailed list of items that can be ordered off-the-shelf (experimental enclosure, cameras, polarization filter, LED light sources, magnets, needles, heater, humidifier, etc.); (2) a detailed list of commercially available electronics/robotics components (servo motors, amplifiers, power adaptors, cables); (3)

custom-made open-source code for the execution of different motor commands enabling defined rotations of the polarization filter; (4) custom-made open-source instructions for 3D-printing of all parts necessary to assemble a functioning virtual flight arena. Taken together, we estimate the cost for assembling such a device (in its most complete version) around 8000 EUR, assuming an existing access to a 3D filament printer. In order to demonstrate the usefulness of this experimental setup, we performed a series of experiments investigating the navigational decisions of individual wild type flies suspended under a rotating polarization filter. In agreement with previous studies, we find that every tested fly chooses a different heading with respect to the incident e-vector field, and tries to maintain this heading when the e-vector is abruptly changed. Importantly, flies show a strong tendency for setting a similar heading during two consecutive trials, even when these were interrupted by a period of unpolarized light. For a more robust quantification of this behavior over time, we introduce a new stimulus, where the e-vector slowly rotates, thereby enabling the fly to continuously adjust its heading in ‘open loop’ conditions. Using this stimulus, we show that the accuracy of the flies’ performance while attempting to keep their chosen heading under such a slowly rotating linearly polarized UV stimulus varies greatly within a population, yet such a behavior is never observed under unpolarized UV light, or linearly polarized green light. Finally, we show that flies that perform well within a 5-minute experiment show a high tendency to choose the same heading in a second experiment, when interrupted by a 5 minute interval of unpolarized light. These experiments underscore the usefulness of the experimental setups presented here and serve as an ‘open source’ platform for the development of new assays optimized for different visual behaviors, in flies as well as other species of flying insects.

Results

The aim of this study was to develop an experimental apparatus for the study of skylight navigation of *Drosophila*, where single flies are glued on a steel needle and suspended in flight via the use of two magnets (magnetotether)[21] under a rotating polarization filter, while flying inside a backlit cylinder (in order to reduce reflection artifacts), being filmed by an infrared camera from below in order to extract the fly's heading.

<u>New modular assays for studying skylight navigation in individual flying flies</u>

Our new virtual flight arenas are assembled from a combination of commercially available parts and custom-designed components that can be 3D-printed using standard filament printers (Figure 1A,B) (see supplemental materials for a list and description of components, as well as materials and methods for printing instructions). One individual assay is fixed on a 30cmx30cm double density optical breadboard (Thorlabs) via two compatible metal beams (Thorlabs). To these, high-power LED light sources with collimated optics (Mightex) can be attached via a 3D printed, horizontal holder (upper holder). LED's are held in place via magnets, to facilitate swapping light sources of different colors (supplemental Figure 1A,B). A robotics-grade servo motor for rotating the polarization filter (Dynamixel MX-28T, Robotis) is attached via a second horizontal holder (lower holder) which is attached to the rotatable filter wheel. The filter wheel contains a 3D-printed gear system as well as two removable cassettes into which polarization filters, diffusers and quarter wave plate retarders can be placed (described in more detail below), in order to produce unpolarized stimuli, or to simulate different degrees of polarization, if desired (Figure 1C). The fly is glued to a steel pin using UV-cured glue and held in place by sapphire bearing and a magnet (the top magnet) attached to a UV fused silica plate that rests in a horizontal platform which is in turn held in place by four vertical metal bars (Figure 1B,D). To extract the animal's body axis, it is filmed using an infrared camera (Firefly MV, Point Grey) pointing upwards (Figure 1B,E), yet shielded from the fly's view via a small box containing infrared LED's, on which rests a round bottom plate containing a pinhole and the bottom magnet (see Figure 1B for magnification). The setup is completed by a white, backlit cylinder containing LED strips for reducing linearly polarized artifacts reflected of the walls of any apparatus. This cylinder can by moved vertically, all the way to the horizontal platform, whenever a new fly needs to be tethered (see Figure 2B). Due to the magnet above the fly, its field of view is somewhat reduced in its center. Similarly to other existing assays, we calculated two areas of unobstructed view each spanning ~28° towards the front and the back of the dorsal visual field (Figure 1E).

<u>Assembly of virtual flight arena from 3D-printed and off-the-shelf parts</u>

In order to result in reproducible data, behavior experiments need to be performed in a stable environment. We therefore placed our behavioral assays within affordable enclosures (Monacor Rack-6W) with enough room to house up to three virtual flight arenas. However, we decided to sacrifice the central spot in favor of an evaporation humidifier (Philips HU4706/11) which can be regulated via an LCD display humidity controller (TMT-HC-210 Humidity Control II). Temperature control is achieved via a PID Temperature Controller driving a 230V carbon heating plate (#100575, Termowelt.de) and two fans mounted on the far side of the enclosure (supplemental Figure 1C). Using this simple design, the enclosure can be stably kept at high temperatures like 32°C, thereby enabling specific heat-dependent genetic manipulations[22].

The modular design of this new virtual flight arena both simplifies assembly, and enables project-specific modifications. Upon first installation, two major parts need to be manually processed: The rotatable filter wheel (Figure 2B) can be printed as a set of 5 parts, including the gear system and assembly is quick and easy. However, we recommend that small steel balls (2 mm) be inserted manually, creating a ball bearing, so that smooth turning is achieved, even at the highest speeds supported by the servo motor, thereby ensuring quick and controlled changes in filter orientation. Similarly, the white cylinder surrounding the flying fly can be 3D-printed in one piece (see supplemental Figure 2), yet LED strips (Paulmann MaxLED 1000) need to be inserted manually into the wall of the cylinder upon first installation.

As a whole, the virtual flight simulator consists of four independently powered steering units (Figure 2C): PID temperature controller, humidity controller, stimulus LED controller, and a laboratory power supply for the white LED strips in the cylinder. These components can easily be coordinated via a switch board (Figure 2A). The recording setup consists of an Arduino-based motor controller (Arbotix-M) which TTL-triggers a free running recording of the two attached cameras via the recording software Streampix 7 (Norpix). Synchronously, the motor controller triggers the motors which rotate the pol-filter (0.088° resolution) and receives positional feedback from the motors.

The camera streams get slightly compressed using MJPEG compression and stored onto the same computer for later image processing and data analysis.

Characterization of the stimulus presentation section

Important controls for testing behavioral responses to linearly polarized light include either (i) depolarizing the stimulus, while keeping its intensity constant[23, 24], or (ii) converting the linearly polarized stimulus into circularly polarized light, which should be perceived as unpolarized, by most if not all insect photoreceptors[25, 26]. We have designed the filter holder of our experimental setup in a way that can quickly and easily accommodate for both kinds of controls, thereby making lengthy adjustments to the experimental design unnecessary. In its assembled state, the rotatable filter holder contains two removable filter cassettes (Figure 3A). The top one contains a bed (5 x 5 cm) into which polarization filter and several sheets of diffuser can be placed, and is overlaid with a round aperture. This filter cassette can easily be removed and inverted, between two experiments, thereby transforming a linearly polarized stimulus into an unpolarized one. The bottom cassette contains a rotatable holder for quarter wave plate (QWP) retarder. Using the internal gear system, the QWP can be placed into different, fixed orientations with regard to the polarization filter, thereby producing elliptically to circularly polarized light, depending on its position. To verify the efficacy of this stimulus presentation system, we have characterized the stimuli emanating from our apparatus using a polarimetric camera[27] (Figure 3B). By calculating the degree of linear polarization as previously described[27], we confirm that the polarized stimuli manifest a high degree of polarization both in the UV (365 nm) as well as with a green LED (510 nm). In contrast, virtually no polarization is detected when the polarization filter / diffuser combination of the upper filter cassette is inverted.

Flying *Drosophila* adjust their heading after rapid switches of the incident e-vector

As a first series of experiments we tested our virtual flight arenas by recording behavioral responses of single flying flies to rapid switches of the incident linearly polarized UV light presented dorsally (PolUV1). In a single experiment, flies were recorded for 5 minutes with the polarized UV stimulus continuously switching back-and-forth between two orthogonal filter positions (termed a and b), every 30 seconds. Upon such rapid 90° changes of the incident polarized stimulus we observed that many flies also showed the tendency to rapidly adjust their flight heading by about 90°, following the filter switch (Figure 4A). On average, a clear increase in the fly's angular velocity was measured shortly after rapid filter switches, indicating robust behavioral responses to changes in the polarization. However, when the same fly was presented with unpolarized UV light of the same intensity as the polarized UV stimulus (UVunpol), the fly did not react to rapid filter rotation, neither by rapidly adjusting its heading, no by increased angular velocity after the switch (Figure 4B). Importantly, when the UV stimulus was repolarized by flipping the upper filter cassette (see Figure 1C and Figure 3A), the above described behavioral responses of the fly to rapid filter switches (adjustment of heading angle; increase of angular rotation) was restored (Figure 4C). When pooling data from all tested flies (N = 69) flying under the above described regime (consecutive 5 min epochs of polarized and unpolarized UV stimuli), flies showed significantly larger angular differences in flight heading between a and b periods when flying under polarized light, as compared to unpolarized trials (Figure 4D). Similarly, the increase in angular velocity shortly after rapid filter switches also differed significantly in flies flying under a linearly polarized UV stimulus, as compared to trials under unpolarized UV light of the same intensity (Figure 4E). Taken together, these findings indicate that single flies flying in our virtual flight arena indeed reacted to changes in e-vector orientation rather than intensity- or other artifacts that could possibly exist within the arena.

Flying *Drosophila* follow a slowly rotating e-vector at an arbitrary angular distance

In order to achieve a more robust quantification of behavioral responses to changes in e-vector orientation (polarotaxis), we introduced a new stimulus: flies flying within the virtual flight arena were presented a linearly polarized stimulus rotating slowly with constant angular velocity (~ 6°/s). In these experiments the 5-minute recording session per trial was split up into 30 x 10s windows. For each of these 30 windows the mean angular velocity of each fly was then calculated. If the difference between this angular velocity and the filter's angular velocity was smaller than 3°/s, the particular time window was categorized as polarotactic behavior (areas shaded grey). For each of these periods the fly's chosen heading was then calculated as the mean angular difference between the fly's body axis and the incident e-vector (blue bar plots). A representative fly (Figure 5A) flying under a constantly rotating e-vector adjusted its heading in about one third of the recorded 10 sec time windows (10/30). The number and length of observed interruptions without polarotaxis varied from fly to fly, resulting in a wide spread of behavioral performance quality (as defined by number of polarotactic

10 sec time windows) when integrating over the entire 5 minutes tested. Importantly, the calculated preferred heading of a given fly falls within a narrow angular range when compared across polarotactic periods (Fly in Figure 5A: mean heading 63.2°, SD=12°), despite interspersed periods of non-polarotactic behavior. This indicated that flies attempt to keep a preferred heading with respect to the celestial e-vector pattern over short periods of time. As expected, virtually no polarotactic periods were detected when the same fly flew under unpolarized UV light (UVunpol), but otherwise unchanged conditions (Figure 5B). Similarly, when the fly was flying under linearly polarized green light (PolGreen), virtually no polarotaxis was detected (Figure 5C). However, upon presenting the fly re-polarized UV light again (PolUV2), polarotactic time periods were restored, in some cases even more pronounced than in the first UV trial (Figure 5D). Pooled data from all tested flies flying under a constantly rotating filter under different lighting conditions (PolUV1, UVunpol, PolGreen, PolUV2) revealed that polarotaxis occurred exclusively when using a linearly polarized UV stimulus (Figure 5E). Flies flying under a slowly rotating linearly polarized UV stimulus spent significantly more time following the e-vector, compared to flying under unpolarized UV or polarized green light, respectively. Interestingly, flies that underwent a second flight under re-polarized UV light spent even a more time following the e-vector. Surprisingly, flies flying under polarized green light showed a weak yet significant response (when compared to unpolarized UV conditions), indicating that the behavioral response may not be completely limited to the UV range, but may also extend to longer wavelengths. Finally, analysis of behavioral responses of female and male flies reveal no significant

differences between genders in the first as well as in a second trial under polarized UV light (PolUV1 and PolUV2).

Chosen headings are arbitrary, while behavioral performance varies between flies

By comparing the behavior across many individuals (N = 66) we investigated the spread of preferred headings when single flies were flying under a slowly rotating polarization filter. The goal was to investigate whether, in this particular kind of virtual flight arena, certain headings are naturally preferred or avoided, or whether the choice of preferred heading is arbitrary and therefore different between individual flies. The strategy is exemplified by the direct comparison of four representative traces of individual flies in response to a slowly rotating polarized UV stimulus (Figure 6A). Quality of behavioral performance (polarotaxis intervals) and preferred heading were quantified as escribed above. It appeared that in these trials each fly chose a different preferred heading with respect to the incident angle of polarization (circular plots). Taken together, the preferred heading angles of all tested flies during their first such linearly polarized UV trial (PolUV1) were distributed over the whole angular range (Fig. 6B,C). Importantly, although the time spent following the rotating e-vector (number of polarotaxis intervals, i.e. quality of behavioral performance) varied greatly between individuals, it did not correlate with the angular heading choice of the animals (Fig. 6D).

Arbitrarily chosen headings are maintained between trials

Finally, we tested whether the amount of time that the flies spent following the e-vector (number of polarotaxis intervals, i.e. quality of behavioral performance) within the first linearly polarized UV trial (PolUV1) correlates with the tendency of the flies to choose a similar preferred heading in a second consecutive trial (PolUV2) that was separated from the first by an interruption (5 min of UVunpol). We found that the better the flies' performance within the first trial (more time spent following the e-vector in PolUV1), the higher the likelihood of them choosing a similar heading in the second trial (Figure 7A). During both PolUV1 and PolUV2 intervals, the probability of tested flies following the rotating e-vector increased during the 5 min trial (Fig.7B). In contrast, the overall lower polarotactic values obtained in control conditions (UVunpol and PolGreen) showed no similar increase over time.

Discussion

Navigating insects rely on the detection and integration of a combination of visual cues, like celestial bodies, intensity, gradients, and chromatic gradients[28]. In addition, the celestial pattern of linearly polarized light serves as an attractive orientation cue that many insects use[29-31]. Spontaneous behavioral responses of both walking and flying *Drosophila* to linearly polarized light ('polarotaxis') have been demonstrated in the past, using both population assays, as well as single fly assays[13-15, 24, 32-34]. In all these experiments, much care was given to the control and avoidance of intensity artifacts that can result in behavioral decisions that are in fact independent of the linearly polarized component of the stimulus (reviewed in[16]). However, some of the successful solutions presented in the past included components whose reproduction required considerable engineering skills and were quite costly. The virtual flight arenas presented here have been designed with the dual goal of providing relatively cheap, robust setups that can easily be assembled, while at the same time minimizing intensity/reflection artifacts. For instance, reflections off the wall of any experimental chamber have been shown to produce intensity patterns that could be used by the animal as a directional cue[16]. Our setup addresses this threat by surrounding the flying fly with a white, backlit cylinder. Furthermore, highly collimated LED light sources were chosen here in order to reduce off-axis illumination which can produce intensity confounds when hitting the polarization filter. The polarimetric characterization of the stimulus used here makes us confident that these effects have been minimized. This is supported by unpolarized UV controls, where the order of polarization filter and diffuser are inversed, which is easy and quick, using the removable, upper filter cassette built into our 3D-printed filter wheel. Single flies flying under a linearly polarized green stimulus also displayed no obvious polarotaxis (yet behaved different from the unpolarized control), which was to be expected due to the fact that polarization-sensitive R7 and R8 photoreceptors in the dorsal rim area (DRA)[35] of the fly eye both express the UV Rhodopsin Rh3[36-38]. Nevertheless, behavioral responses to linearly polarized stimuli with longer wavelengths have also been reported in the past[13, 24], which raises the question what kind of retinal detectors are responsible[24, 39]. In addition to different combinations of polarization filters, diffusers, and band pass filters, our system can also be equipped with a quarter wave plate (QWP) / retarder that can be rotated into varying fixed orientations with respect to the polarization filter (lower filter cassette). Such an introduction of a QWP is particularly useful for testing behavioral performance while simulating different degrees of polarization[25, 26]. Although the degree of polarization in nature never reaches the high values normally used in the laboratory, data so far available only for crickets points towards the polarotactic responses to be stable across a range of degrees of polarization[25, 26, 40].

Using our new virtual flight arenas, we show that individual flies choose arbitrary headings under a linearly polarized stimulus, and in sum all chosen headings appear to spread randomly. This finding is in good agreement with recently published studies, albeit using a rather different kind of stimulation system[15]. In further agreement with these past studies, we also find that flies show a clear tendency to keep their chosen heading, even when interrupted by a period of unpolarized stimulation[15]. These data further support the idea that a generalist fly like *Drosophila melanogaster* is indeed capable of using skylight polarization for navigational tasks[17]. We propose that quantifying the quality of a behavioral response by chopping a 5-minute experiment under the slowly rotating polarization filter into 30 sec polarotactic periods serves as an attractive new strategy for producing statistically significant data in a reasonable amount of time. Nevertheless, our experiments also show that behavioral responses remain variable across all individuals tested. Even after tight control of food quality, rearing conditions, temperature, and humidity, the flies' cooperation in these experiments remains unpredictable. How much this variability could depend on the fly's motivational state or navigational decision making remains to be investigated.

We are in the process of making all the codes, templates and building instructions for the virtual flight arenas freely available for download to anyone (see materials and methods). Due to their modular design, the use of our new virtual flight assays is in no way limited to skylight navigation or the study of polarized light vision. With few simple modifications they could be modified for studying behavioral responses to moving stimuli, color patterns, or celestial bodies. Similarly, the setups can easily be modified to house a spherical treadmill, for studying the visual behavior in walking flies. Finally, application is in no way limited to just *Drosophila* or other small flies. We hope that the assays presented here can serve as a platform from which many other assays optimized for many other species could evolve from.

Methods

Fly rearing

An Isogenized strain of Oregon R flies[41] was fed standard cornmeal agarose food and kept at 25°C and 60% relative humidity within a 12/12 light/dark cycle. Flies were flipped daily to ensure small population densities.

Fly preparation

All experiments were conducted during the evening peak of the flies' entrained activity rhythms reaching until one hour after subjective "sunset". 3-4 days old flies were immobilized using cooling with ice and individual flies were then glued to a 1cm long 100µm diameter steel (ENTO SPHINX s.r.o., Czech Republic) pin using UV-cured glue (Bondic). The pin was attached to the fly so that when positioned vertically it held the animal at an angle pointing approximately 60° from horizontal. During the gluing procedure flies were placed onto a peltier-element set to about 4°C to keep flies immobilized. Before each experiment, flies were given at least 20 minutes to recover and were kept from flying by placing small pieces of tissue paper (Kimwipes) at their tarsi. To initiate flight for data acquisition a small air puff was given to the flies immediately from below using bellows. Flies that stopped flying more than 3 times within one trial of 5 minutes were excluded from later analysis.

Flight simulator setup

In order to study the skylight navigation in flying *Drosophila melanogaster* we modified the setup by Weir and Dickinson[14]. We created a highly modular, easy to replicate behavioral assay and placed two identical copies of this assay into one optical enclosure in order to increase the rate of data output. Most functional parts of this setup were 3D printed which allows for easy replication of the setup, when having access to a 3D printer.

Fly tethering

The setup allows flies to be positioned within an axially-symmetric magnetic field created by magnets above (cylinder magnet, 4x 4mm x 5mm) and below (ring magnet, 10mm x 5mm, inner diameter 5mm) the fly, allowing the animal to freely rotate around its yaw axis. The side of the upper magnet that was facing the fly was covered with a small white plastic cap. The upper magnet was held in place at the center of a 50mm diameter UV fused silica Window by placing another small magnet (cylinder magnet, 5mm x 5mm) at the other side of the window. A small sapphire jewel bearing was attached to the center of this cap. This bearing served to hold the tip of the steel pin with the fly in place. The lower magnet was centrically glued to the bottom of a rough white plastic platform, hiding the magnet from the view of the fly. A 5mm hole at the center of this bottom plate allowed for delivering air puffs and also recording the fly through that hole.

Image acquisition

For imaging the fly's rotation and determining its heading, a camera suitable for fast near-infrared imaging (Firefly MV, Point Grey) was placed upwards so that it imaged through the hole in white bottom platform. The camera's objective was screwed to a small chamber at the bottom of the base plate. This chamber served as a spacer to increase the distance between the camera and the fly in order to match the focal range of the objective relative to the position of the fly. Furthermore, a 5mm diameter hole at the side of this chamber allowed for connecting the bellows and giving air puffs to the animal. Also, this chamber served as a housing for four infrared LEDs (880nm, 100mA max) which were placed directly onto a long-pass filter (#87C, Lee filters) centered on top of the objective lens with putty, but avoiding a small region directly at the center of the objective, allowing for the fly still to be imaged through that hole. The infrared light from the LEDs projected upwards through the hole in the bottom base plate, illuminating the fly for proper imaging while being invisible to the fly itself.

Stimulus delivery

Above the UV fused silica window which holds the upper magnet in place, a custom designed freely rotatable Filter holder was installed. This holder allows for insertion of two tightly fitting filter cassettes. The upper cassette held a combination of a 50mm x 50mm sheet linear polarizer (OUV5050, Knight Optical, UK) and 13 layers of thin, non-fluorescent diffuser paper (80g/sqm, Max Bringman KG) and could be inserted into the rotatable cassette holder with either the polarizer or the diffuser side facing the fly. This setup allowed for presenting the fly either linearly polarized or unpolarized light dorsally, depending on which side of the filter cassette was facing the fly, providing a way to alter the degree of polarization while maintaining the light intensity. The rotatable filter cassette holder was held in place by a manually assembled ball bearing. This was done by modelling a 2.15mm gap between the filter cassette holder and its surrounding frame when constructing the 3D models. This gap was sparsely lubricated, almost completely filled with 2mm diameter steel balls and covered with a fitting top plate to keep the balls in place. The rotatable filter cassette holder contained a gear system (template created using https://geargenerator.com) which was driven by a 360° servo motor capable of sending positional feedback data (MX-28T, Dynamixel). The servo was controlled with an Arduino-compatible microcontroller (Arbotix-M, Trossen Robotics) allowed for precise rotations of the filter cassette holder and with it the angle of the e-vector of linearly polarized light. To illuminate the fly through the polarizer/diffuser either a collimated UV (365nm, LCS-0365-13-B, Mightex) or a collimated green (530nm, LCS-0530-15-B, Mightex) LED were mounted centrally above the filter cassette holder, projecting light through the filters and to the ventral side of the fly's eye. The intensity of the two LEDs was set approximately isoquantaly to $2x10^{12}$ photons/s/cm2 using a spectrometer (Flame, Ocean Optics).

Motor control of filter rotation

Data acquisition was synchronized using the Arbotix-M microcontroller which controlled motor position and triggered the infrared camera. For recording videos, we used Streampix software (Norpix). With this software it was possible to monitor the input state of one of the digital I/O connections of the camera to trigger and end a free running recording. The input state was defined by a TTL signal emanating from the Arbotix-M in order to synchronize video acquisition with motor movements. Images were acquired with 60 frames per second in greyscale and 640x480 pixel resolution and stored in M-JPEG compressed AVI files. Two different types of motor command programs were created and tested: (1) rapid switches (see Figure 4) and (2) continuous rotation (see Figures 5 and 6). The rapid switching protocol consisted of rapidly rotating the E-vector by 90°, keeping it static for 30s and then rapidly switching it back by 90° to its original position. The duration of a 90° switch was approximately 1s. This rotational pattern was repeated 10 times, resulting in a duration of recording of ~5min. In order to better describe time periods where the flies kept following the E-vector, the continuous rotation stimulus was created. This protocol consisted of rotating the E-vector with constant angular velocity (5.97 deg/s) for 5 minutes.

Extraction of flight heading

Tracking of the fly's body axis angle was done offline using the open-source software Fiji. To automate this process a macro was created for Fiji which opens all relevant AVI files in a folder, separates the fly from the background, performs per-frame tracking and saves the tracked angular data of the fly's heading to a text file. The macro involves an automated rolling ball background subtraction, a median filter to smooth out pixel noise and a thresholding command to binarize the image and separate the fly's body from the background. Afterwards, Fiji fitted an ellipse around the fly's body in each frame, outputting the angular data of the heading of the fly over time from 0° to 180°. Due to the directional ambiguity of the E-vector we also calculated the E-vector angle within a range from 0° to 180°. The text files containing the tracking results for each frame of a video were later analyzed using MatLab.

Open access

Files necessary for 3D-printing flight simulator parts, as well as codes and further assembly instructions will become available in the coming days, under:

www.flygen.org/skylight-navigation

References

1. Paulk, A., Millard, S.S. & van Swinderen, B. Vision in Drosophila: seeing the world through a model's eyes. *Annu Rev Entomol* **58**, 313-332 (2013).
2. Stowers, J.R. *et al.* Virtual reality for freely moving animals. *Nat Methods* **14**, 995-1002 (2017).
3. Frye, M.A. & Dickinson, M.H. Closing the loop between neurobiology and flight behavior in Drosophila. *Curr Opin Neurobiol* **14**, 729-736 (2004).
4. Vogel, S. Flight in Drosophila. II. Variations in stroke parameters and wing contour. *J Exp Biol* **46**, 383-392 (1967).
5. Gotz, K.G. Flight control in Drosophila by visual perception of motion. *Kybernetik* **4**, 199-208 (1968).
6. Rister, J. *et al.* Dissection of the peripheral motion channel in the visual system of Drosophila melanogaster. *Neuron* **56**, 155-170 (2007).
7. Tuthill, J.C., Nern, A., Holtz, S.L., Rubin, G.M. & Reiser, M.B. Contributions of the 12 neuron classes in the fly lamina to motion vision. *Neuron* **79**, 128-140 (2013).
8. Melnattur, K.V. *et al.* Multiple redundant medulla projection neurons mediate color vision in Drosophila. *J Neurogenet* **28**, 374-388 (2014).
9. Liu, G. *et al.* Distinct memory traces for two visual features in the Drosophila brain. *Nature* **439**, 551-556 (2006).
10. Theobald, J.C., Shoemaker, P.A., Ringach, D.L. & Frye, M.A. Theta motion processing in fruit flies. *Front Behav Neurosci* **4** (2010).
11. Aptekar, J.W., Shoemaker, P.A. & Frye, M.A. Figure tracking by flies is supported by parallel visual streams. *Curr Biol* **22**, 482-487 (2012).
12. Giraldo, Y.M. *et al.* Sun Navigation Requires Compass Neurons in Drosophila. *Curr Biol* **28**, 2845-2852 e2844 (2018).
13. Wolf, R., Gebhardt, B., Gademann, R. & Heisenberg, M. Polarization Sensitivity of Course Control in Drosophila-Melanogaster. *J Comp Physiol* **139**, 177-191 (1980).
14. Weir, P.T. & Dickinson, M.H. Flying Drosophila Orient to Sky Polarization. *Current Biology* **22**, 21-27 (2012).
15. Warren, T.L., Weir, P.T. & Dickinson, M.H. Flying Drosophilamelanogaster maintain arbitrary but stable headings relative to the angle of polarized light. *J Exp Biol* **221** (2018).
16. Foster, J.J. *et al.* Polarisation vision: overcoming challenges of working with a property of light we barely see. *Naturwissenschaften* **105**, 27 (2018).
17. Dickinson, M.H. Death Valley, Drosophila, and the Devonian toolkit. *Annu Rev Entomol* **59**, 51-72 (2014).

18. Katsov, A.Y. & Clandinin, T.R. Motion processing streams in Drosophila are behaviorally specialized. *Neuron* **59**, 322-335 (2008).

19. Baden, T. *et al.* Open Labware: 3-D printing your own lab equipment. *PLoS Biol* **13**, e1002086 (2015).

20. Maia Chagas, A., Prieto-Godino, L.L., Arrenberg, A.B. & Baden, T. The euro100 lab: A 3D-printable open-source platform for fluorescence microscopy, optogenetics, and accurate temperature control during behaviour of zebrafish, Drosophila, and Caenorhabditis elegans. *PLoS Biol* **15**, e2002702 (2017).

21. Bender, J.A. & Dickinson, M.H. Visual stimulation of saccades in magnetically tethered Drosophila. *J Exp Biol* **209**, 3170-3182 (2006).

22. Simpson, J.H. Mapping and manipulating neural circuits in the fly brain. *Adv Genet* **65**, 79-143 (2009).

23. Brunner, D. & Labhart, T. Behavioral Evidence for Polarization Vision in Crickets. *Physiol Entomol* **12**, 1-10 (1987).

24. Wernet, M.F. *et al.* Genetic dissection reveals two separate retinal substrates for polarization vision in Drosophila. *Curr Biol* **22**, 12-20 (2012).

25. Henze, M.J. & Labhart, T. Haze, clouds and limited sky visibility: polarotactic orientation of crickets under difficult stimulus conditions. *J Exp Biol* **210**, 3266-3276 (2007).

26. Labhart, T. How polarization-sensitive interneurones of crickets perform at low degrees of polarization. *J Exp Biol* **199**, 1467-1475 (1996).

27. Ilic, M., Meglic, A., Kreft, M. & Belusic, G. The Fly Sensitizing Pigment Enhances UV Spectral Sensitivity While Preventing Polarization-Induced Artifacts. *Front Cell Neurosci* **12**, 34 (2018).

28. Heinze, S. Unraveling the neural basis of insect navigation. *Curr Opin Insect Sci* **24**, 58-67 (2017).

29. Mathejczyk, T.F. & Wernet, M.F. (Oxford Encyclopedia of Neuroscience, 2017).

30. Labhart, T. & Wehner, R. Polarization Vision, in *Invertebrate Vision*. (eds. E.J. Warrant & D.E. Nilsson) 291-348 (Cambridge University Press, Cambridge; 2006).

31. Wehner, R. Polarization vision--a uniform sensory capacity? *J Exp Biol* **204**, 2589-2596 (2001).

32. Weir, P.T. *et al.* Anatomical Reconstruction and Functional Imaging Reveal an Ordered Array of Skylight Polarization Detectors in Drosophila. *J Neurosci* **36**, 5397-5404 (2016).

33. Velez, M.M., Gohl, D., Clandinin, T.R. & Wernet, M.F. Differences in neural circuitry guiding behavioral responses to polarized light presented to either the dorsal or ventral retina in Drosophila. *J Neurogenet* **28**, 348-360 (2014).

34. Velez, M.M., Wernet, M.F., Clark, D.A. & Clandinin, T.R. Walking Drosophila align with the e-vector of linearly polarized light through directed modulation of

angular acceleration. *J Comp Physiol A Neuroethol Sens Neural Behav Physiol* **200**, 603-614 (2014).

35. Labhart, T. & Meyer, E.P. Detectors for polarized skylight in insects: a survey of ommatidial specializations in the dorsal rim area of the compound eye. *Microsc Res Tech* **47**, 368-379 (1999).

36. Fortini, M.E. & Rubin, G.M. The Optic Lobe Projection Pattern of Polarization-Sensitive Photoreceptor Cells in Drosophila-Melanogaster. *Cell and Tissue Research* **265**, 185-191 (1991).

37. Fortini, M.E. & Rubin, G.M. Analysis of Cis-Acting Requirements of the Rh3 and Rh4 Genes Reveals a Bipartite Organization to Rhodopsin Promoters in Drosophila-Melanogaster. *Gene Dev* **4**, 444-463 (1990).

38. Wernet, M.F. *et al.* Homothorax switches function of Drosophila photoreceptors from color to polarized light sensors. *Cell* **115**, 267-279 (2003).

39. Heinloth, T., Uhlhorn, J. & Wernet, M.F. Insect Responses to Linearly Polarized Reflections: Orphan Behaviors Without Neural Circuits. *Front Cell Neurosci* **12**, 50 (2018).

40. Wehner, R. & Labhart, T. Polarization vision. *Invertebrate vision*, 291-348 (2006).

41. Silies, M. *et al.* Modular use of peripheral input channels tunes motion-detecting circuitry. *Neuron* **79**, 111-127 (2013).

Acknowledgements

The authors thank Tanja Heinloth, Lena Naber and Nurelhoda Abdel Muti for experimental support, as well as all members of the Wernet and Hiesinger groups for their input. This work was supported by DFG grant WE5761/2-1 and collaborative research grant SFB958 (Teilprojekt A23), the Berlin-based excellency cluster NeuroCure, as well as AFOSR grant FA9550-19-1-7005.

Author contributions

TM and MFW planned the experiments. TM built the assay and performed all experiments. TM and MFW designed the figures. MFW wrote the manuscript, MFW and TM finalized the manuscript.

Figure Legends

Figure 1: A new modular assay for studying skylight navigation in individual flying flies

A. Schematic drawing of a fully assembled virtual flight arena for the quantitative study of skylight navigation in flying *Drosophila*. Commercially available parts include: (1) a 30cmx30cm double density optical breadboard (Thorlabs); (2) compatible metal beams (Thorlabs); (3) swappable, magnetically attached high-power LED light sources with collimated optics (Mightex); (4) a robotics-grade servo motor for rotating the polarization filter (Dynamixel MX-28T, Robotis); (5) an infrared camera shielded from the fly's view, filming its body axis (Firefly MV, Point Grey). Custom-designed 3D-printed parts (see supplemental materials for printing instructions) include: (6) attachment to the vertical bars; (7) filter holder including gear system (see Figures 2 and 3 for details); (8) horizontal platform holding the UV fused silica plate and top magnet for attaching the magnetotethered fly (see Figure 1B for magnification); (9) infrared illumination (enclosed LED's) and bottom plate with ring magnet, mounted onto the infrared camera; (10) backlit cylinder for reducing linearly polarized reflection artifacts, which can be lifted all the way to the horizontal platform, when flies are tethered. **B.** Magnification of central components; from top to bottom: (1) LED light source; (2) polarization filter and diffuser, mounted together within the rotatable filter holder (see Figures 2 and 3); (3) UV fused silica plate for attaching the magnetotether; (4) top magnet; (5) steel pin with fly attached; (6) ground plate with bottom ring magnet below; (7) encased infrared LED's for illumination of the fly's contours; (8) point grey camera for filming the fly's body axis. **C.** Two polarization filter / diffuser orientations can be chosen within the filter holder:

Unpolarized (diffused; top), or polarized (bottom). See Figure 3B for polarimetric characterization. **D.** Example of fly tethered in apparatus. **E.** Series of images visualizing the extraction of the fly's boy axis from camera images. **F.** Drawing of the fly's field of view inside the apparatus.

Figure 2: Assembly of virtual flight arena from 3D-printed and off-the-shelf parts

A. Photograph depicting two fully assembled virtual flight arenas. (1) temperature- and humidity-controlled enclosure (Monacor Rack-6W); (2) PID Temperature Controller; (3) Stimulus LED controller (BLS-SA04-US, Mightex); (4) Humidity controller; (5); Laboratory power supply; (6) LCD display Humidity controller; (7) Switchable power bank; (8) humidifier (Philips HU4706/11); for a complete list of parts, see supplemental materials. **B.** Magnified view of 3D-printed parts. Top: Stimulation section. (1) servo motor; (2) attachment to vertical beams; (3) filter holder (for more details see Figure 3A); (4) gear system for rotating the filter holder; (5) ball bearing enabling smooth rotation. Bottom: modular arrangement of magnetotethered fly: (6) ground plate; (7) mounted infrared camera; (8) ground plate through which fly is filmed; (9) backlit cylinder containing white LED-strips for providing uniform visual environment without polarized reflections can be moved vertically around the near-infared camera / magnetotether via 4 metal guides. **C.** Summary of the four modules interacting within the apparatus (see supplemental materials). **D.** Diagram depicting information flow (For details and codes, see supplemental materials).

Figure 3: Characterization of the stimulus presentation section

A. Modular depiction of the filter holder and its individual components: (1) view of the assembled, rotatable filter holder; (2) Removable top cassette; (3) removable bottom cassette; (4) place holder; (5) round aperture; (6) filter bed (5 x 5 cm); (7) top plate of bottom cassette; (8) rotatable holder for quarter wave retarder plate; (9) body of bottom cassette. **B.** Polarimetric characterization of stimuli as they emanate from the above apparatus. Top: UV stimulus, 370 nm (from left to right: intensity, as well as the two filter/diffuser orientations shown in Figure 1C: polarized (center) and unpolarized (right). Bottom: Same analysis for a linearly polarized green stimulus (510 nm).

Figure 4: Flying *Drosophila* react to rapid switches of the incident e-vector

A. Flight heading (blue line) of a single fly orienting to a linearly polarized UV stimulus (UVpol) that is rapidly changing, every 30 seconds by 90 degrees (from position ‘a’ to position ‘b’ and back). 5 consecutive series (a/b) are shown. Bottom left: circular plot of all heading angles (‘whole’), or separated by polarization filter orientation (‘a’ and ‘b’ periods, respectively). Bottom, center: mean heading of ‘a’ and ‘b’ periods, and difference between the two. Bottom, right: plot showing the speed difference (in degrees per s) 10 s before and after the rapid polarization filter switch. **B.** Same analysis for an unpolarized UV stimulus (‘UV unpol’), directly following the above experiment (same fly). **C.** Same analysis for a re-polarized UV stimulus (‘UVpol’), directly following both above experiments (same fly). **D.** Mean angular difference between a and b epochs for all tested flies. The mean angular difference between a and b is significantly higher under polarized UV light compared to flies flying under unpolarized UV light. Consecutive trials alternating between polarized and unpolarized UV conditions show polarotactic responses can be elicited and prevented and that the linear polarization of light is necessary and sufficient for this behavior. *p<0.05, **p<0.01, ***p<0.001. N (left to right) = 16,16,13,13,11. **E.** Difference in angular speed between mean speed 10s before and 10 s after rapidly switching the e-vector for all tested flies. The difference in angular speed is significantly higher under polarized UV light compared to flies flying under unpolarized UV light. Consecutive trials alternating between polarized and unpolarized UV conditions show the necessity and sufficiency of polarized light in inducing a turning tendency shortly after rapid e-vector switching. *p<0.05, **p<0.01, ***p<0.001n. N (left to right) = 16,16,13,13,11.

Figure 5: Flying *Drosophila* follow a slowly rotating e-vector at an arbitrary angle

A. Left: Flight heading (blue line) of a single fly orienting to a slowly rotating linearly polarized UV stimulus (PolUV1; orange line). 30 s intervals with above threshold polarotactic behavior (see material and methods) are shown in grey. Right: plot of above threshold intervals and circular plot of heading chosen by the animal. **B.** Same analysis as above, using an unpolarized UV stimulus (UVunpol); same fly. **C.** Same analysis as above, using a polarized green stimulus (PolGreen); same fly. **D.** Same analysis as above, using a re-polarized UV stimulus (PolUV2); same fly. **E.** Summary plot of % time spent following the slowly rotating e-vector, comparing the four conditions from above (N (from left to right = 66, 22, 38, 43). **F.** Direct comparison of male versus female polarotaxis from PolUV1 and PolUV2 experiments reveals no significant difference (N (from left to right) = f30, m36, f19, m24).

Figure 6: Chosen headings are arbitrary, while behavioral performance is variable

A. Flight heading (blue line) of four single flies orienting to a slowly rotating linearly polarized UV stimulus (PolUV1; orange line). 30 s intervals with above threshold polarotactic behavior (see material and methods) are shown in grey. Right: plot of above threshold intervals and circular plot of heading chosen by the animals. **B.** Summary of heading angles (angular difference to the polarization filter) chosen by 66 individual flies, under the PolUV1 stimulus. **C.** Same data plotted on circular coordinates reveals a wide distribution. **D.** Same data as in B where behavioral performance (% of time following the e-vector) is represented in false color.

Figure 7: Arbitrarily chosen headings are maintained between trials

A. Plot depicting the angular difference between headings chosen in two consecutive trials interrupted by a period of unpolarized light (PolUV1 vs PolUV2) as a function of the quality of polarotaxis during the PolUV1 period (% of time spent following e-vector). B. The change of polarotaxis probability over the 5 min experimental time window, plotted for all 4 experimental conditions (PolUV1, UVunpol, PolGreen, and PolUV2).

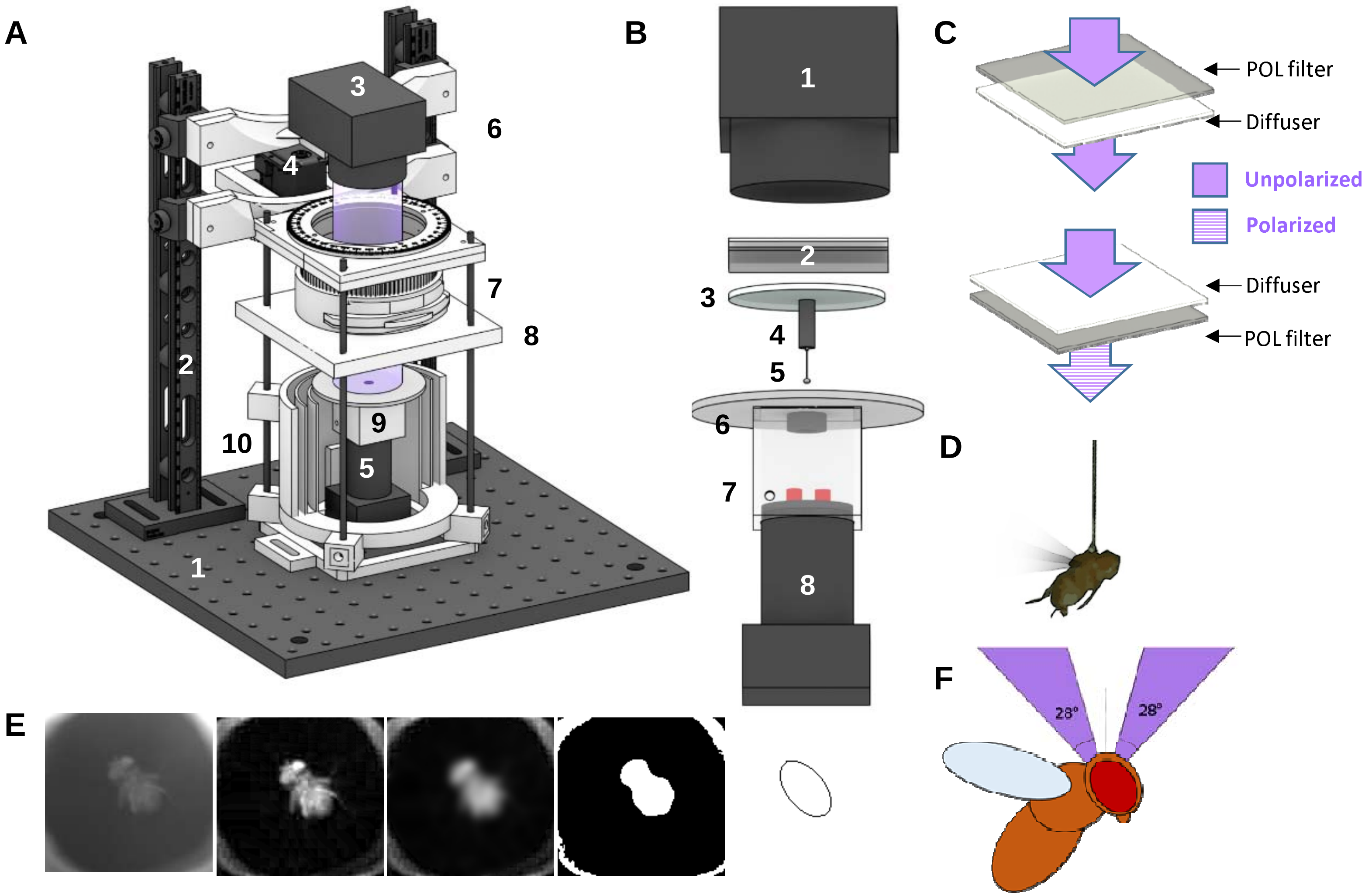
A
1
2
3
4
5
6
7
8
9
10
B
1
2
3
4
5
6
7
8
C
POL filter
Diffuser
Unpolarized
Polarized
Diffuser
POL filter
D
E
F
28°
28°

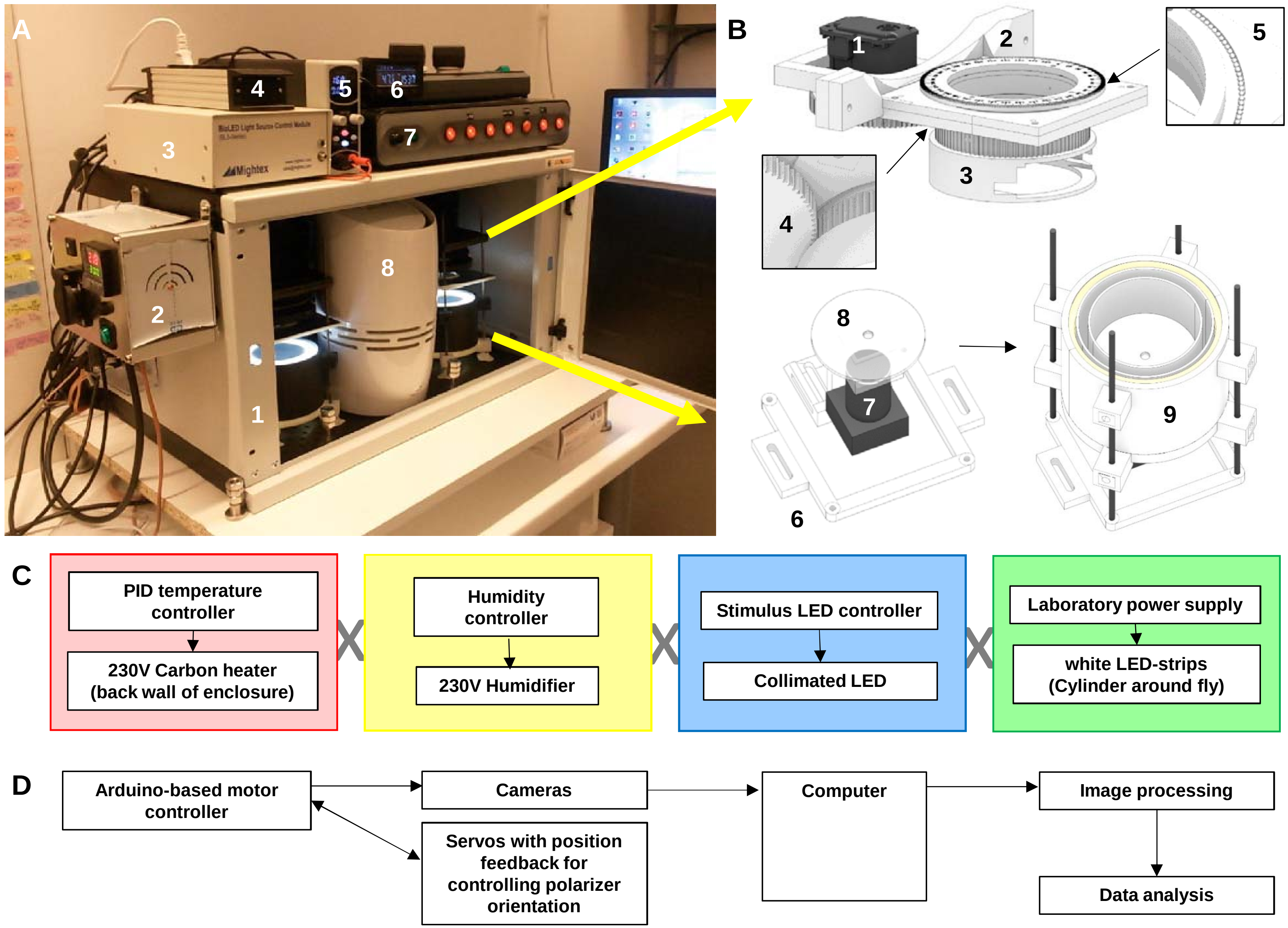
A
4
5
6
3
7
Mightex
8
2
1
B
1
2
5
3
4
8
7
9
6
C
PID temperature controller
230V Carbon heater (back wall of enclosure)
Humidity controller
230V Humidifier
Stimulus LED controller
Collimated LED
Laboratory power supply
white LED-strips (Cylinder around fly)
D
Arduino-based motor controller
Cameras
Servos with position feedback for controlling polarizer orientation
Computer
Image processing
Data analysis

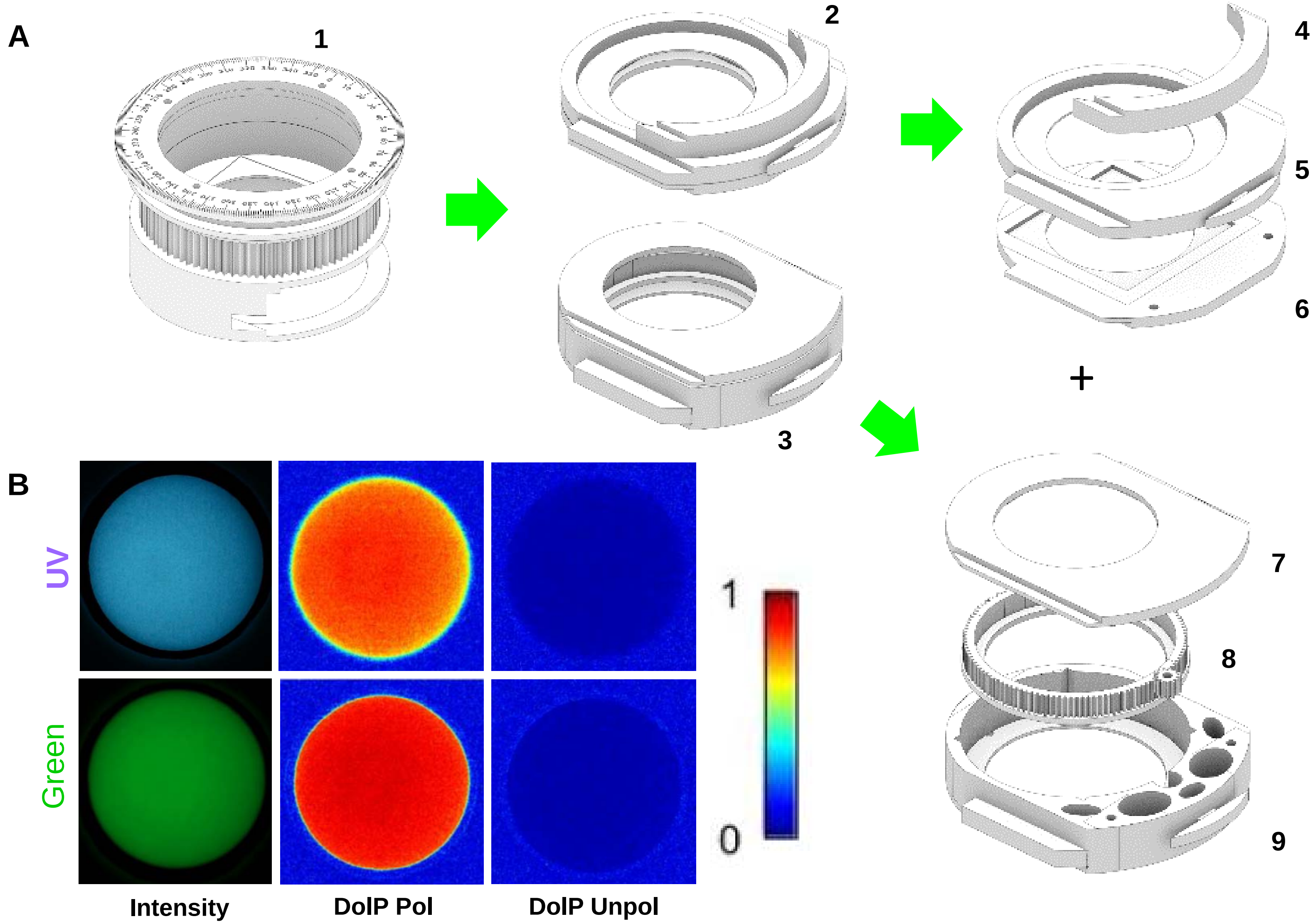
A
1
2
3
4
5
6
+
7
8
9
B
UV
Green
1
0
Intensity
DolP Pol
DolP Unpol

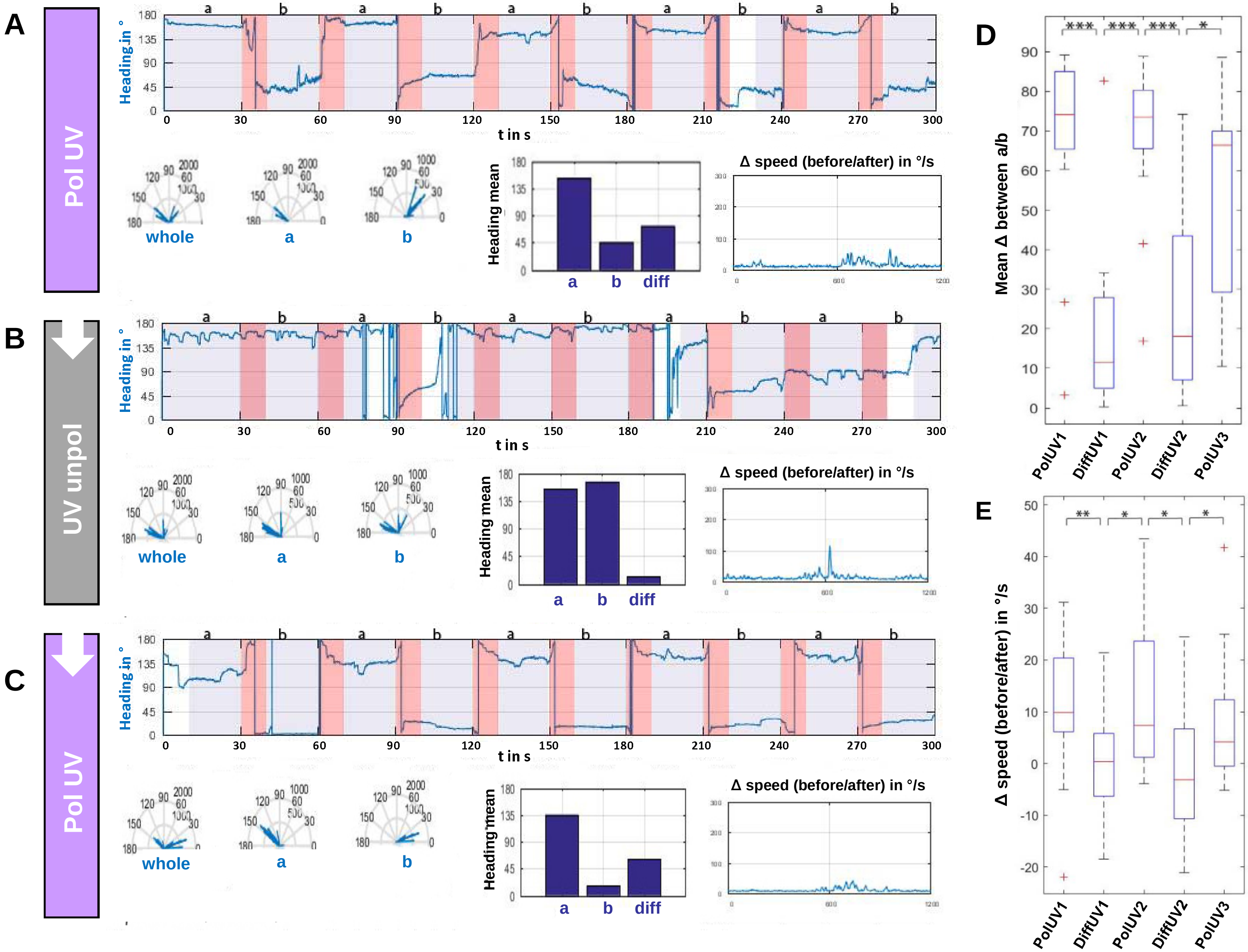
A
Pol UV
B
UV unpol
C
Pol UV
Heading in °
t in s
whole
a
b
Heading mean
diff
Δ speed (before/after) in °/s
D
Mean Δ between a/b
PolUV1
DiffUV1
PolUV2
DiffUV2
PolUV3
E
Δ speed (before/after) in °/s

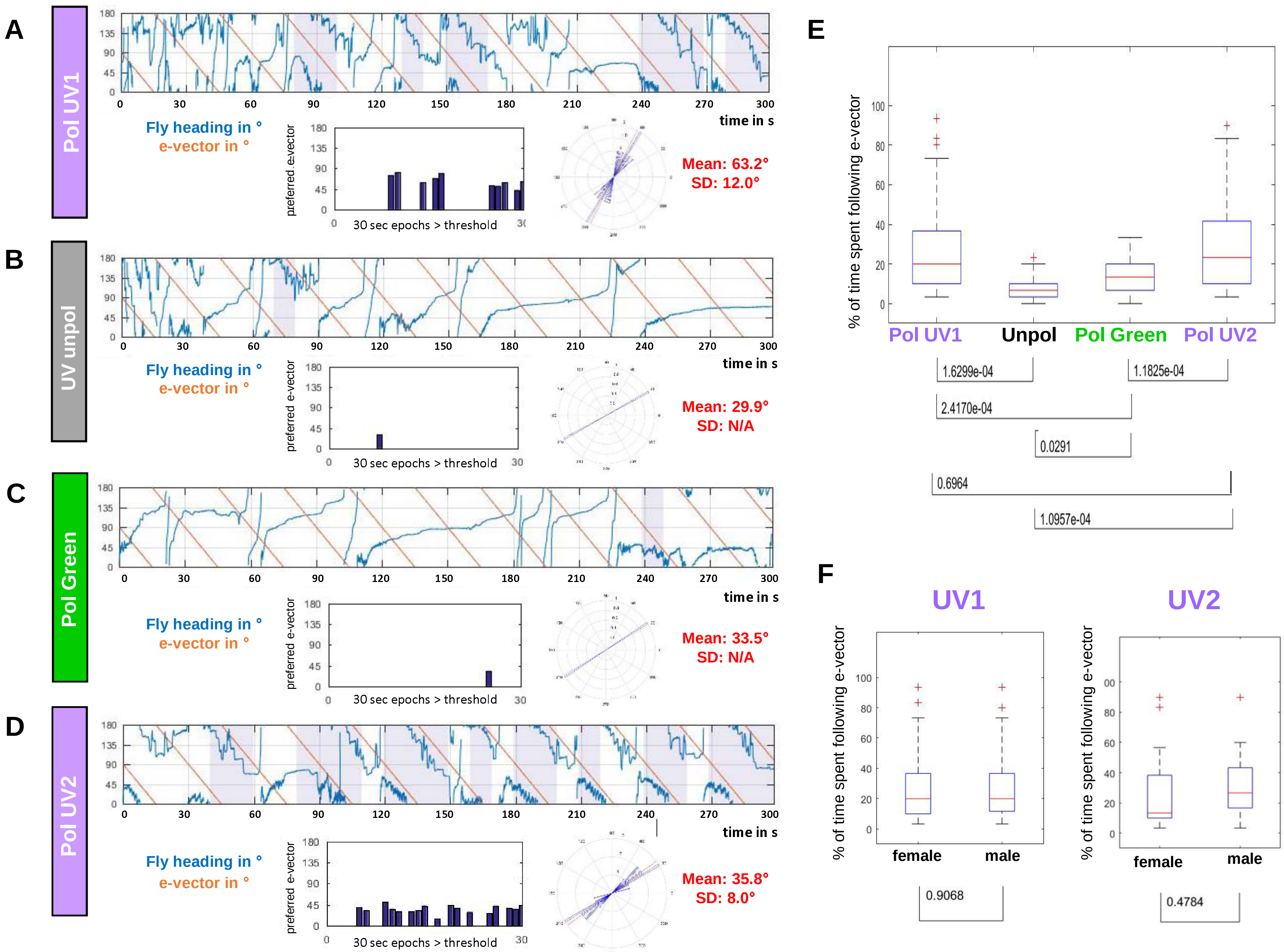
A
Pol UV1
Fly heading in °
e-vector in °
time in s
preferred e-vector
30 sec epochs > threshold
Mean: 63.2°
SD: 12.0°
B
UV unpol
Fly heading in °
e-vector in °
time in s
preferred e-vector
30 sec epochs > threshold
Mean: 29.9°
SD: N/A
C
Pol Green
Fly heading in °
e-vector in °
time in s
preferred e-vector
30 sec epochs > threshold
Mean: 33.5°
SD: N/A
D
Pol UV2
Fly heading in °
e-vector in °
time in s
preferred e-vector
30 sec epochs > threshold
Mean: 35.8°
SD: 8.0°
E
% of time spent following e-vector
Pol UV1
Unpol
Pol Green
Pol UV2
1.6299e-04
1.1825e-04
2.4170e-04
0.0291
0.6964
1.0957e-04
F
UV1
UV2
% of time spent following e-vector
female
male
0.9068
0.4784

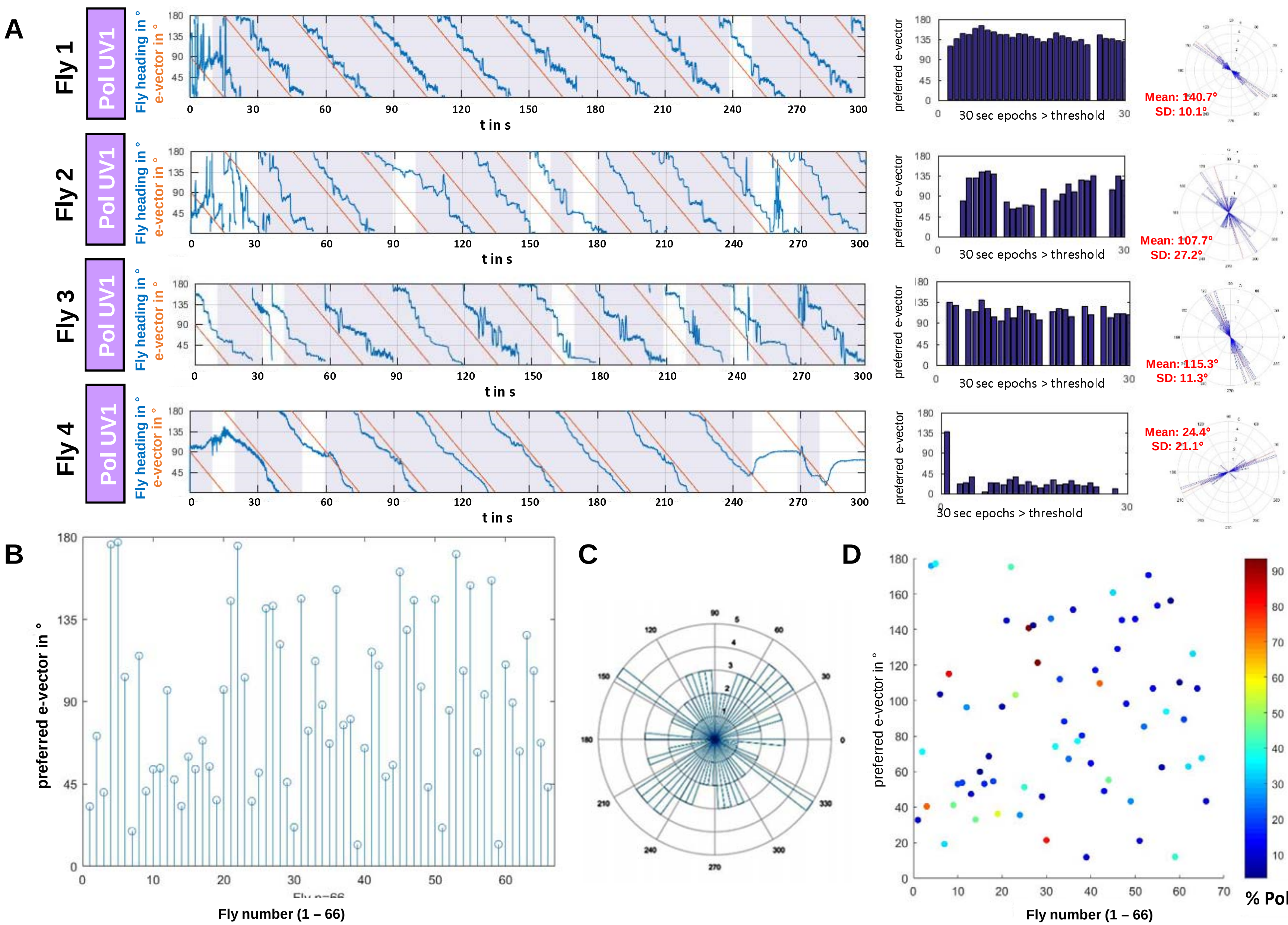
A
Fly 1
Fly 2
Fly 3
Fly 4
Pol UV1
Fly heading in °
e-vector in °
t in s
preferred e-vector
30 sec epochs > threshold
Mean: 140.7°
SD: 10.1°
Mean: 107.7°
SD: 27.2°
Mean: 115.3°
SD: 11.3°
Mean: 24.4°
SD: 21.1°
B
preferred e-vector in °
Fly number (1 – 66)
C
D
preferred e-vector in °
Fly number (1 – 66)
% Pol

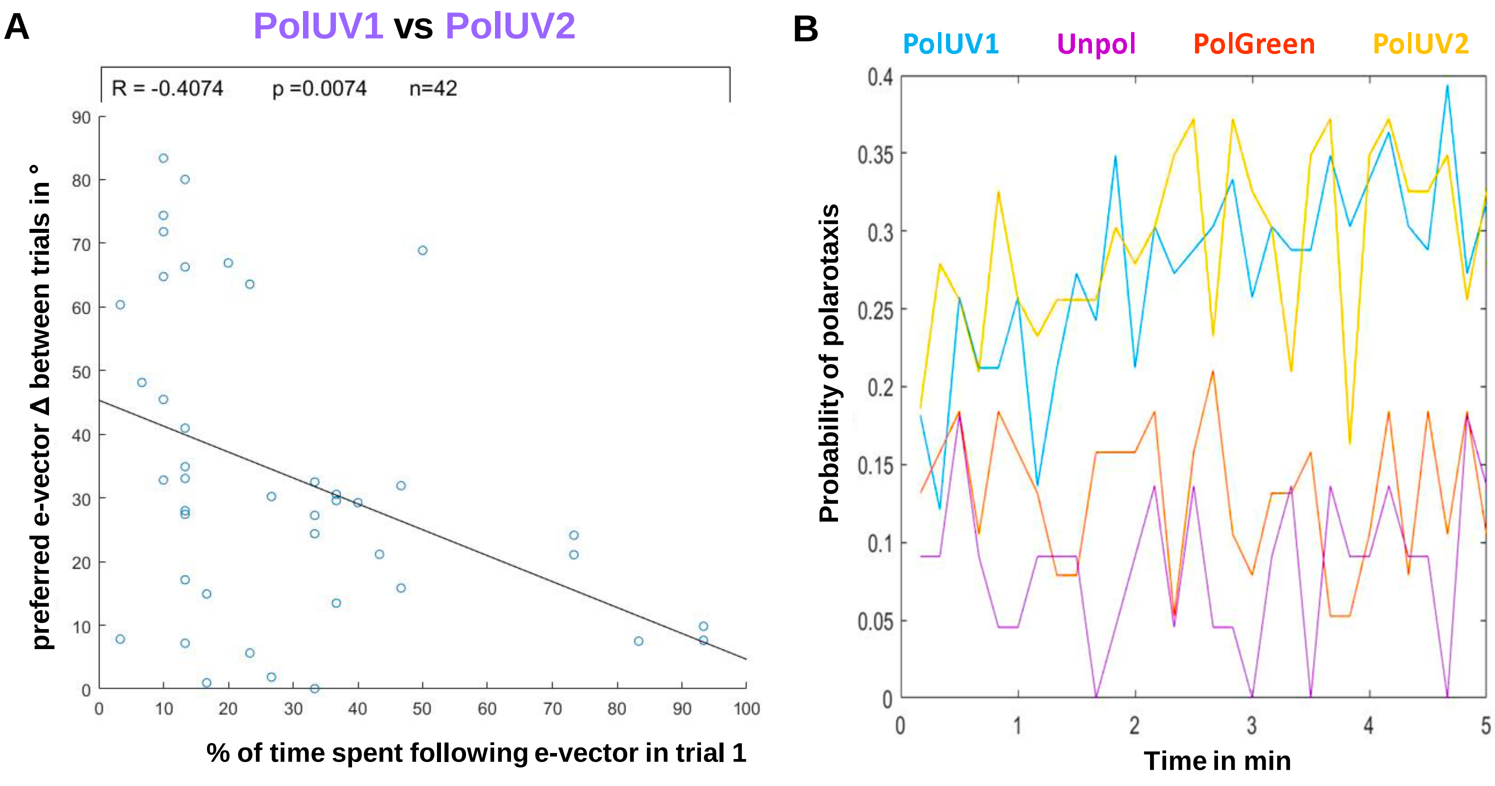
A
PolUV1 vs PolUV2
R = -0.4074 p =0.0074 n=42
preferred e-vector Δ between trials in °
% of time spent following e-vector in trial 1
B
PolUV1
Unpol
PolGreen
PolUV2
Probability of polarotaxis
Time in min